OPTIMIZED PASSIVE DEVICES FOR LOW-POWER LNA DESIGN

Ignacio Gil*, Raúl Fernández
Departament d'Enginyeria Electrònica
Universitat Politècnica de Catalunya (UPC)
08222 Colom 1, Terrassa, Spain
*e-mail: gilgali@eel.upc.edu

Javier J. Sieiro, José M. López-Villegas
Departament d'Electrònica
Universitat de Barcelona (UB)
08028 Martí i Franquès 1, Barcelona, Spain
e-mail: sieiro@el.ub.es

***Abstract*—This paper addresses the design of high-Q passive inductors and differential transformers in a low-power low-noise amplifier (LNA) application. The passives quality in resonant LC tanks as well as in the matching network and degeneration inductors has been improved by balancing the trade-off between ohmic losses and Eddy current degradation. As a result, the enhanced passives Q-factor for the optimized passive devices has been used in order to design a 2.4 GHz fully integrated high-gain current-reused LNA, implemented in 0.18 µm CMOS technology. The LNA performance show a gain of roughly 30 dB, while dissipating 0.9 mA from a 1.2 V supply.**

***Index Terms*—Low-power, LNA, Q-factor, ISM-band**

I. INTRODUCTION

The impact of passives quality in resonant circuits can severely influence the circuit power dissipation [1]. In conventional low-noise amplifiers (LNAs) the load inductor is typically used to resonate with a certain fixed capacitance in order to obtain the specified peak voltage gain, A_V. This gain is proportional to the tuned circuit's impedance at resonance, Z_o and transistor's transconductance, g_m. Z_o is usually limited by the inductor quality factor, Q, since $Z_o \propto Q$. Thus, the voltage gain behavior is described by means of

$$A_V \propto g_m Q. \qquad (1)$$

LNA stage has been deeply analyzed in literature, and straightforward figures of merit (*FoMs*) have been given as

$$FoM_{LNA} = \frac{A_V \, IIP3 \, f}{(NF-1)P}. \qquad (2)$$

where *IIP3* is the input-referred third-order intercept point, *NF* the noise figure, *P* the DC dissipated power and *f* the operating frequency. Assuming (2), to lower power dissipation the RF CMOS technology is scaled down, since the evolution of defined FoM_{LNA} almost increases inversely with the minimum gate length, *Lmin*, because of in short channel regimes $f_T \propto 1/Lmin$ [2]. In fact a clear trend toward better LNA performance for reduced designed CMOS technology nodes is observed in the literature and, more specifically, from the low-power design point of view [3]. Therefore, according (1), to compensate the reduction of g_m and A_V due to low-power requirements, the passives quality factor must be increased. In this work, the design of a 2.4 GHz fully integrated CMOS high-gain low-power LNA is carried out by means of high-Q passive devices. A single-ended to differential current-reused topology is proposed. All the used passive inductors and transformers have been optimized in two ways: first to obtain the best balance between ohmic and Eddy current losses, second to achieve an improved routing solution in terms of layout. Specially, the impact of high-Q LC tanks and inductors is analyzed and discussed.

II. LNA IMPLEMENTATION

The schematic of the designed LNA is illustrated in Fig. 1. A 50 Ω π-matching network formed by capacitors C_1, C_2 and inductor L_G, followed by a decoupling capacitor C_{in} and a pseudo-differential configuration formed by transistor pair *M1-M2* is performed. ESD protection diodes equivalent capacitance corresponds to C_1 and C_2. The capacitance *C'* allows to minimize the noise figure under low-power conditions and degeneration inductor, L_S, completes the matching network. In order to obtain a fully differential RF amplified signal in *M1* and *M2* drain, a bypass capacitor, C_{diff}, copies the signal between the two nodes by preserving the DC component. The RF signal goes through two decoupling capacitances, C_{int}, to a second common- source transistor pair *M3-M4*. By combining an optimized differential transformer, *T1*, with two shunt capacitors, C_{T1}, an improved RF-choke is implemented between the two stacked transistor pairs. Optimized differential transformers are the key in order to enhance the quality factor of the LC tank resonance. As result, the overall NF is decreased since the gain of the input

This work has been partially by the *Spanish Ministerio de Ciencia e Innovación* under projects TEC2009-09994 and the *AGAUR* of the *Generalitat de Catalunya* (2009SGR-1425).

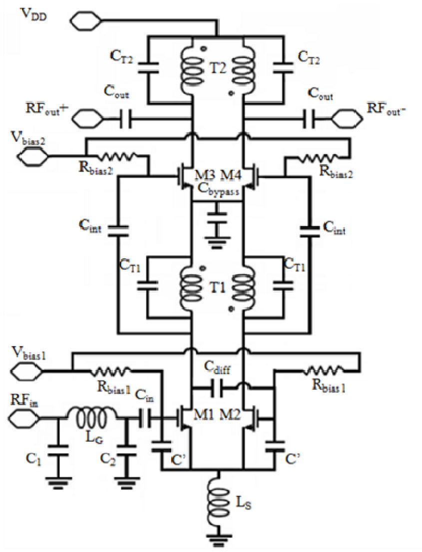

Fig. 1. Schematic of the single-ended to differential current-reused LNA.

stage is enhanced and the noise contribution of *M3-M4* is minimized. The insertion of extremely high-quality passives make possible to improve LNA performance, not only from the power consumption point of view, but also in order to have excellent chokes for reducing RF leakage between *M3-M4* sources and *M1-M2* drains, respectively. This structure reduces common mode noise since the up and down-conversion even harmonics are suppressed, as well. According to the small-signal equivalent circuit of the LNA, the differential voltage gain at the tank's resonance is given by

$$A_V = -\frac{\dfrac{2g_m}{1-\omega^2 L_S C'_{gs}}}{j\omega C'' + \dfrac{2}{R_L}}, \qquad (1)$$

where $$C'_{gs} = C_{gs} + C'; \;\; C'' = \frac{C_{diff} C'_{gs}}{C_{diff} + C'_{gs}}. \qquad (2)$$

At resonance, the impedance of the transformer is reduced to a real load, R_L. Impedance behaviour equivalent to that of a shunt configuration formed by *C''* and half of the transformer appears in the gain, which indicates that the tank's resonance is dependent on C_{diff}. Therefore, as explained above, the importance of the passives quality is directly pointed out through *T1* and L_S, since there is a direct relationship with A_V. Moreover, the term $L_S C'_{gs}$ must be carefully considered since it can generate a resonance at $f=1/(L_S C'_{gs})^{1/2}$ which could potentially lead to oscillations and circuit instability. The amplifier stability is discussed in section IV. A large bypass capacitor, C_{bypass}, connected to the *M3-M4* sources provides a reliable AC ground. A second LC tank (formed of a differential transformer, *T2*, and capacitors C_{T2}) is designed as an improved RF-choke and short for common mode in order to resonate at the desired frequency (2.4 GHz @ ISM-band) in combination with the output capacitance, C_{out}. In that case the high quality of the passives leads to an optimized load which enhances the device gain with no extra power dissipation. Biasing resistor networks are included by means of R_{bias1} and R_{bias2} resistances. Note that *M1* and *M3* branch shares the same bias current (which takes the same value as in the symmetric *M2* and *M4* branch). This merged structure reduces DC current with a significant power consumption saving for the overall implementation.

III. PASSIVES DESIGN

A. Inductors

The overall integrated inductor losses can be divided in substrate losses and strip metal losses. Although substrate losses are a critical factor degrading the performance of Si integrated RF inductors, in this work we have considered a conventional Si substrate, since the application requirements correspond to a standard CMOS process (with no possibility of silicon removal). Concerning metal strip losses, two main contributions show up: ohmic losses and magnetically induced losses. The former are related to conduction currents whereas the latter are due to Eddy currents induced on the inductor coil. A trade-off dependant on the width of the inductor's metal strip appears, since ohmic losses are minimized for wider metals whereas minimum metal areas decrease magnetically induced currents. In order to optimize the Q-factor of the RF inductors, their central turns width is reduced (Eddy currents is the dominant effect) and the external turns are widen (ohmic losses are dominant). The final layout of the inductors has been derived in order to minimize the overall losses by means of the systematic optimization method detailed in [4]. The procedure is based on computing the conduction losses and the loss associated with the Eddy currents, but maintaining the inductance value and the available area as constraints. The resulting geometry is a tapered spiral with narrower strips in the inner turns and wider trips in the external ones, as explained above. The electromagnetic simulations have been performed by using the *Agilent Momentum* software based on the method of moments. Both, experimental and simulated results have been obtained from S-parameters extraction and transformation to Y-parameters, according:

$$L_{eff} = \frac{im(1/Y_{11})}{\omega}, \quad Q = \frac{-im(1/Y_{11})}{re(1/Y_{11})}. \qquad (3), (4)$$

The LNA design requirements include an inductor for the input matching network, L_G (=10nH), and a degeneration inductor L_S (=1nH), depicted in Fig. 2. Due to the fact that both inductors are in the single-ended signal path coming from the antenna, they have been laid out as square spirals. Fig. 3 shows the experimental Q and effective inductance values for both inductors. As can be observed the measured results at 2.4GHz correspond to L_G=10.49nH, $Q_p(L_G)$=16.2, L_S=1.07nH, $Q_p(L_S)$=13.4, whereas maximum tested quality factor correspond to $Q_{peak}(L_G)$=17 and $Q_{peak}(L_S)$=33 at higher frequencies, respectively.

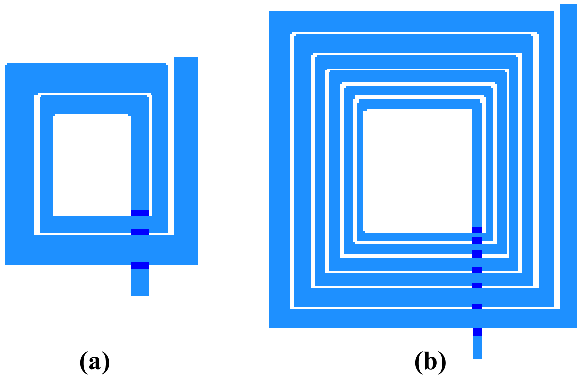

Fig. 2. Optimized implemented inductors. (a) L_S=1nH. Dimensions correspond to 200x200 µm^2. (b) L_G=10nH. Dimensions correspond to 310x310 µm^2.

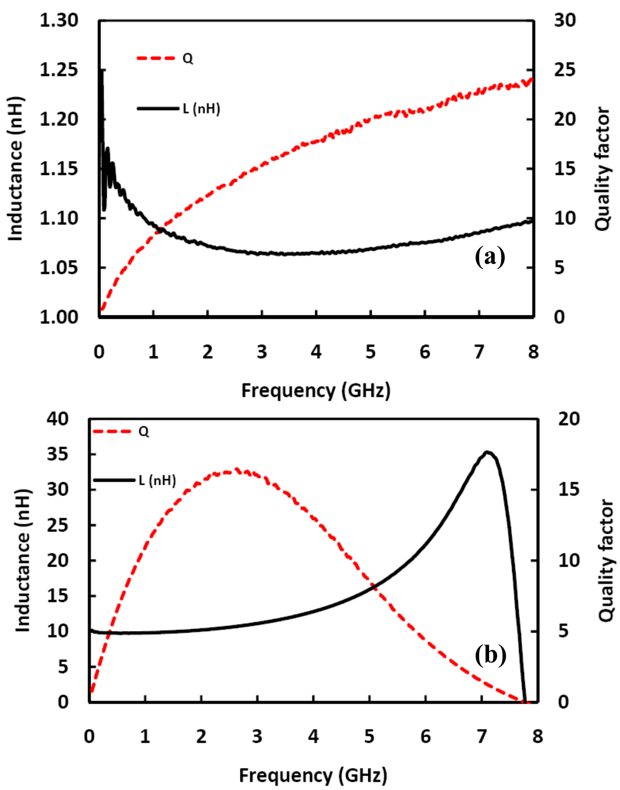

Fig. 3. Experimental Q and inductance of the designed inductors. (a) L_S=1nH. (b) L_G=10nH.

B. *Differential Transformers and LC-tanks*

The LNA is implemented by two transformers LC-tanks, as shown in Fig. 1. These resonant structures have three main functions. First, they provide a way for reusing the bias current for the LNA. Second, they must be able to force a short impedance condition for the common-mode signal and, therefore, the even harmonics at the output of the LNA are suppressed. Third, they offer a high impedance condition (high gain) for the differential mode. Such behaviour can be accomplished when the magnetic coupling factor k between transformer windings is close to -1 (inverter configuration) in

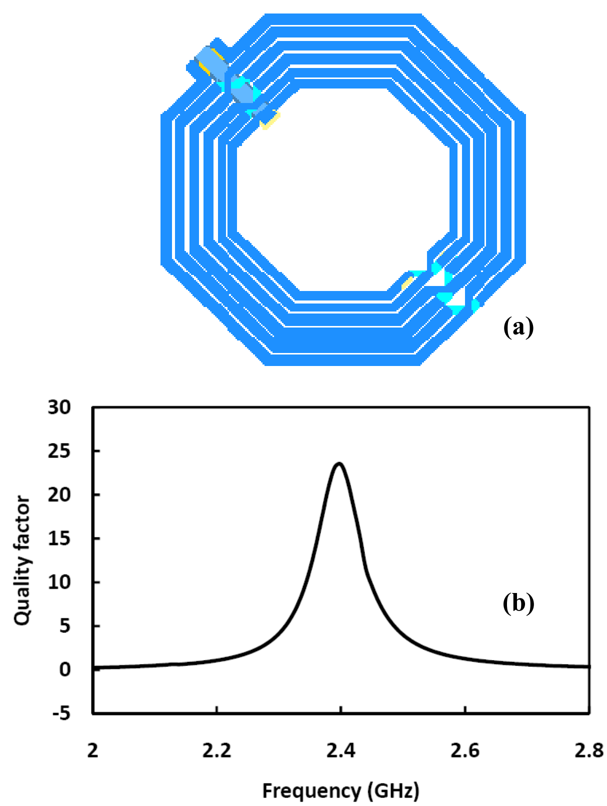

Fig. 4. (a) Differential optimized transformer and (b) LC-tank Q-factor.

combination with a high quality factor of the passive component. The high impedance condition can be set through the equivalent parallel resonance. Thus, in such cases, the quality factor will be evaluated using the derivative of the phase θ of the LC-tank at its resonance frequency ω_0, i.e.,

$$Q = \left|\frac{\omega}{2}\frac{d\theta}{d\omega}\right|_{\omega=\omega_0} = \left|\frac{\omega}{2}\frac{d}{d\omega}\left(\tan^{-1}\left(\frac{im(Y_{diff})}{re(Y_{diff})}\right)\right)\right|_{\omega=\omega_0} \quad (5)$$

where Y_{diff} represents the differential admittance of the load connected at the drain outputs of transistors M1-M2 or M3-M4.

To achieve this required functionality, the inverter transformer LC-tank must be carefully designed. In order to minimise the distance to the transistor drain, the layout is octagonal, as shown in Fig. 4(a), with the 3 ports located in the same corner forming a 45º angle. Notice that the shunt capacitors C_T that fix the resonance frequency are placed just at the output of the ports. In this way, the parasitic magnetic couplings due to additional routing traces are avoided. The coupling between windings can be maximized using the minimum separation between metal strips and interleaving the metals forming the two coils as much as possible. Additionally, the high impedance condition for the differential mode can be obtained by increasing Q. Therefore, the former systematic optimization procedure can be applied (notice that both transformers are also tapered structures).

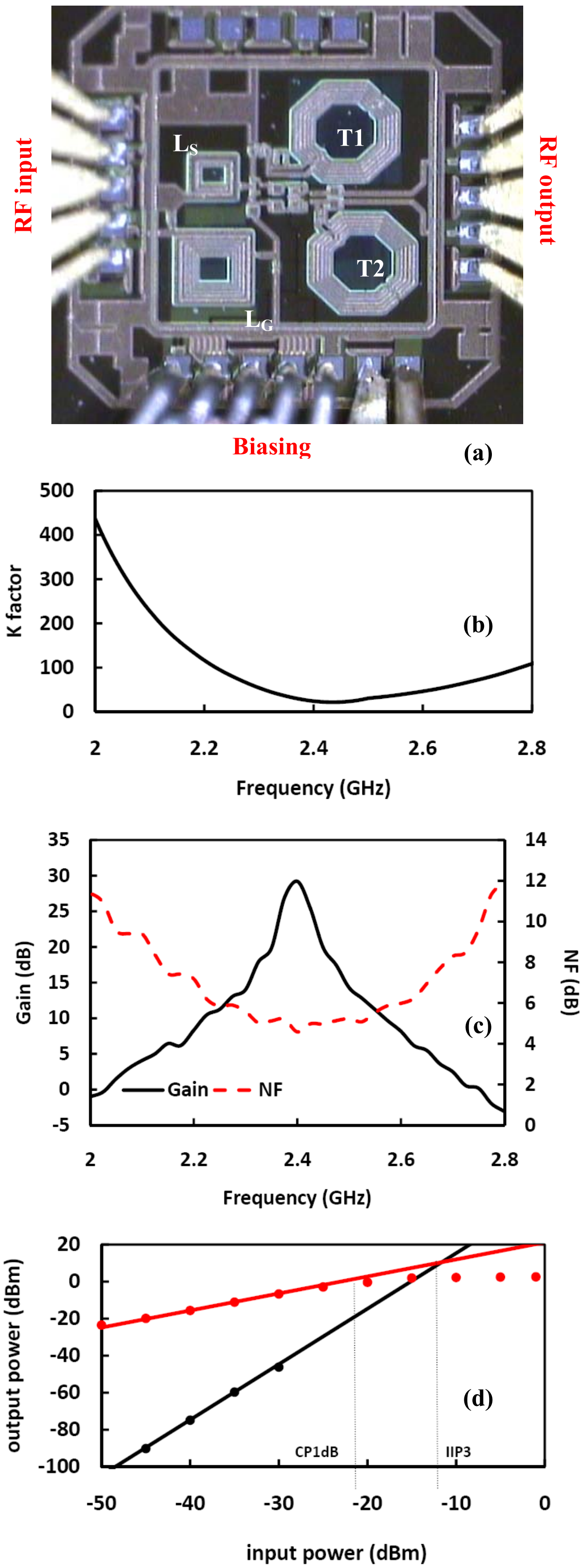

Fig. 6. (a) Tested LNA. (b) LNA Rollet's factor. (c) Measured gain and noise figure. (d) Measured CP1 dB and IIP3.

Using (5), the simulated Q value is 22.5 at the frequency of interest, as shown in Fig. 4(b). The impact of the process variations on the performance has been estimated in a ±6% at resonance frequency, which can potentially degrade the effective Q at resonance frequency. In order to minimise the overall area of the circuit, the two transformer LC-tanks must be placed as close as possible to each other. However, the magnetic and electric coupling between them can modify the resonance frequency of the structures, detuning the high impedance condition for the differential signal.

IV. Experimental Results

Fig. 6(a) shows the implemented LNA. In order to assure amplifier stability under any load condition the Rollet's factor, K, has been simulated. As can be observed in Fig. 6(b), $K>1$ for all the interest frequency range. Therefore, the amplifier is unconditionally stable. Fig. 6(c) shows a LNA experimental gain of roughly 30 dB at central frequency band (2.4 GHz), whereas noise figure corresponds to 4.5 dB. Fig. 6(d) shows the measured nonlinearity effects such as the 1-dB compression point (CP1dB=-21.0 dBm) and the input third-order intercept point (IIP3=-11.5 dBm) of the LNA. In order to evaluate the impact of the ESD diodes on the linearity of the LNA an IIP3 simulation with and without ESD diodes (using equivalent capacitance) has been performed. The simulated LNA without ESD diodes presents CP1dB=-14.2 dBm and IIP3=-5.4 dBm. Finally, the total current consumption of the proposed LNA is 0.9 mA from a 1.2 V supply.

V. Conclusions

The overall strip metal losses of several RF inductors and differential transformers have been optimized in order to obtain high-Q passive devices. Such passives have been used in the design of a single to differential current-reused LNA with the result of high-gain (~30dB) and low-power consumption (~1mW).

Acknowledgment

The authors would like to thank to SEIKO EPSON for the facilities and sample provision.

References

[1] A.A. Abidi, G.J. Pottie and W.J. Kaiser, "Power-conscious design of wireless circuits and systems", Proceedings of the IEEE, vol. 88, pp. 1528–1545, October 2000.

[2] R. Brederlow, W. Weber, J. Saurerer, S. Donnay, P. Wambacq, M. Vertregt, "A mixed-signal design roadmap", IEEE Design and Test of Computers, vol. 18, pp. 34–46, Nov/Dec 2001.

[3] K. Lee, I. Nam, I. kwon, J. Gil, K. Han, S. Park and B.-I. Seo "The impact of semiconductor technology scaling on CMOS RF and digital circuits for wireless application", IEEE Transactions on Electron Devices, vol. 52, pp. 1415–1522, July 2005.

[4] J. M. López-Villegas, J. Samitier, C. Cané, P. Losantos, J. Bausells, "Improvement of the quality factor of RF integrated inductors by layout optimization", IEEE Transactions on Microwave Theory and Techniques. vol. 49, pp. 76–83, January 2000.